RESEARCH   **Open Access**

Cascaded reconstruction network for compressive image sensing

Yahan Wang, Huihui Bai* , Lijun Zhao and Yao Zhao

Abstract

The theory of compressed sensing (CS) has been successfully applied to image compression in the past few years, whose traditional iterative reconstruction algorithm is time-consuming. Fortunately, it has been reported deep learning-based CS reconstruction algorithms could greatly reduce the computational complexity. In this paper, we propose two efficient structures of cascaded reconstruction networks corresponding to two different sampling methods in CS process. The first reconstruction network is a compatibly sampling reconstruction network (CSRNet), which recovers an image from its compressively sensed measurement sampled by a traditional random matrix. In CSRNet, deep reconstruction network module obtains an initial image with acceptable quality, which can be further improved by residual reconstruction network module based on convolutional neural network. The second reconstruction network is adaptively sampling reconstruction network (ASRNet), by matching automatically sampling module with corresponding residual reconstruction module. The experimental results have shown that the proposed two reconstruction networks outperform several state-of-the-art compressive sensing reconstruction algorithms. Meanwhile, the proposed ASRNet can achieve more than 1 dB gain, as compared with the CSRNet.

Keywords: Compressive sensing, Sampling net, Reconstruction net, CSRNet, ASRNet
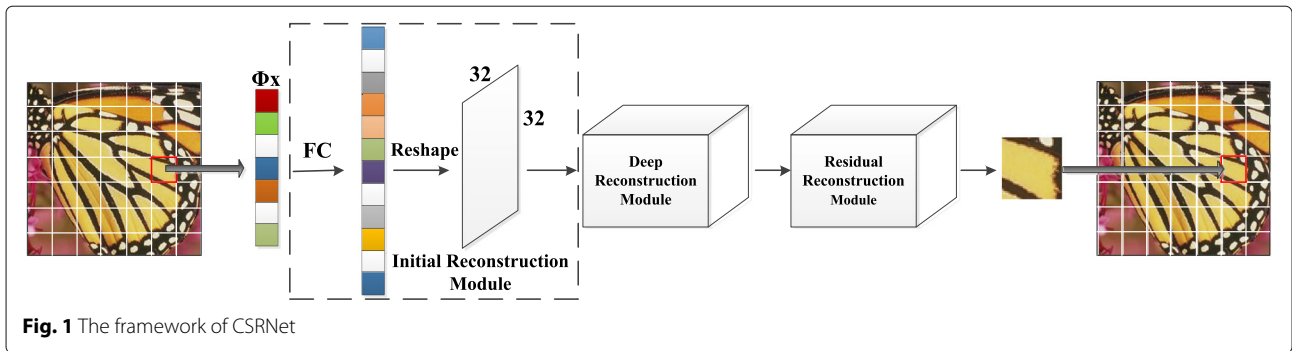
1   Introduction

In the traditional Nyquist sampling theory, the sampling rate must be at least twice of the signal bandwidth in order to reconstruct the original signal losslessly. On the contrary, compressive sensing (CS) theory is a signal acquisition paradigm, which can sample a signal at sub-Nyquist rates but realize the high-quality recovery [1]. Later, Gan et al. proposed block compresses sensing to reduce the algorithm's computational complexity to avoid directly applying CS on images with large size [2]. Due to CS's excellent performance on sampling, CS has already been widely used in a great deal of fields, such as communication, signal processing, etc.

In the past decades, CS theory has advanced considerably, especially in the development of reconstruction algorithms [3–10]. Compressive sensing reconstruction aims to recover the original signal $x \in R^{n \times 1}$ from the compressive sensing measurement $y \in R^{m \times 1}(m \ll n)$. The CS measurement is obtained by $y = \Phi x$, where $\Phi \in R^{m \times n}$ is a

CS measurement matrix. The process of reconstruction is highly ill-posed, because there exist more than one solutions $x \in R^{n \times 1}$ that can generate the same CS measurement y. To solve this problem, the early reconstruction algorithms always assume the original image signal has the property of l_p-norm sparsity. Based on this assumption, several iterative reconstruction algorithms have been explored, such as orthogonal matching pursuit (OMP) [3] and approximate message passing(AMP) [4]. Distinctively, the extension of the AMP, denoising-based AMP (D-AMP) [5], employs denoising algorithms for CS recovery and can get a high performance for nature images. Furthermore, many works incorporate prior knowledge of the original image signals, such as total variation sparsity prior [6] and KSVD [7], into CS recovery framework, which can improve the CS reconstruction performance. Particularly, TVAL3 [8] combines augmented Lagrangian method with total variation regularization, which is also a perfect CS image reconstruction algorithm. However, almost all these reconstruction algorithms require to solve an optimization problem. Most of those algorithms need hundreds of iterations, which inevitably leads to high

Wang *et al. EURASIP Journal on Image and Video Processing* (2018) 2018:77

Page 2 of 16

Fig. 1 The framework of CSRNet

computational cost and becomes the obstacle for the applications of CS.

In recent years, some deep learning-based methods have been introduced into the low-level problems and get excellent performance, such as image super-resolution [11, 12], image artifact removal [13], and CS image reconstruction [14–17]. Recently, some deep network-based algorithms for CS image reconstruction have been proposed. ReconNet is proposed in [14], which takes CS measurement of image patch as input and outputs its corresponding image reconstruction. Especially, for patch-based CS measurement, ReconNet, inspired of SRCNN [11], can retain rich semantic contents at low measurement rate as compared to the traditional methods. In [15], a framework is proposed to recover images from CS measurements without the need to divide images into small blocks, but there is no competitive advantage for the performance of the reconstruction compared with other algorithms. In [16, 17], the residual convolutional neural network is introduced in the image reconstruction for compressive sensing, which can preserve some information in previous layers and also can improve the convergence rate and accelerate the training process. Different from the optimization-based CS recovery methods, the neural network-based methods often directly learn the inverse mapping from the CS measurement domain to original image domain. As a result, it effectively avoids expensive computation and achieves a promising image reconstruction performance.
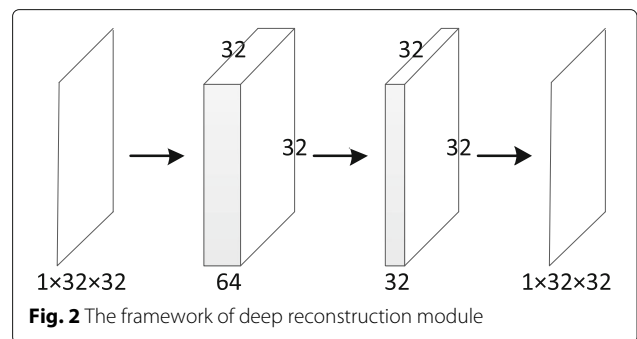
In this paper, two different cascaded reconstruction networks are proposed to meet different sampling methods. Firstly, we propose a compatibly sampling reconstruction network (CSRNet), which is employed to reconstruct high-quality images from compressively sensed measurements sampled by a random sampling matrix. In CSRNet, deep reconstruction network module can obtain an initial image with acceptable quality, which can be further improved by residual network module based on convolutional neural network. Secondly, in order to improve the sampling efficiency of CS, an automatically sampling module is designed, which has a fully connected layer
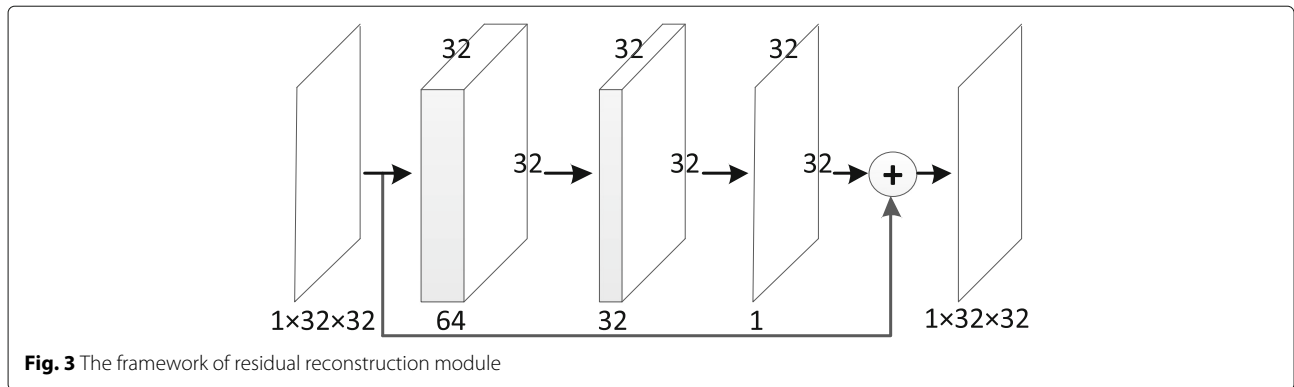
to learn a sampling matrix automatically. In addition, the residual reconstruction module is presented, which can match the sampling module. Both the sampling module and its matching residual reconstruction module form a complete compressive sensing image reconstruction network, named ASRNet. As compared with CSRNet, ASRNet can achieve more than 1 dB gain. The experimental results demonstrate the proposed networks outperform several state-of-the-art iterative reconstruction algorithms and deep-learning-based approaches in objective and subjective quality.

The rest of this paper is organized as follows. In Section 2, two novel networks are proposed for different sampling methods. In Section 3, the performance of the proposed networks is examined. We conclude the paper in Section 4.

2 The methods of proposed networks

In this section, we describe the proposed two networks CSRNet in Fig. 1 and ASRNet in Fig. 4. The first network, CSRNet, is designed to reconstruct image from the CS measurement sampled by a random matrix. The second one is a complete compressive sensing image reconstruction network, ASRNet, consisting of both sampling and reconstruction module. Here, our sampling module contains only one fully-connected layer (FC), which is more powerful to imitate traditional Block-CS sampling process.

Fig. 2 The framework of deep reconstruction module

Wang *et al. EURASIP Journal on Image and Video Processing*   (2018) 2018:77

Page 3 of 16

Fig. 3 The framework of residual reconstruction module

2.1 CSRNet

Our proposed CSRNet consists of three modules, initial reconstruction module, deep reconstruction module, and residual reconstruction module. The initial reconstruction module takes the CS measurement y as input and outputs a B×B-sized preliminary reconstructed image. As shown in the Fig. 1, the deep reconstruction module takes the preliminary reconstructed image as input and outputs a same-sized image. The deep reconstruction module contains three convolutional layers, shown in Fig. 2. The first layer generates 64 feature map with 11×11 kernel. The second layer uses kernel of size 1×1 and generates 32 feature maps. And the third layer produces one feature map with 7×7 kernel, which is the output of this module. All the convolutional layers have the same stride of 1, without pooling operation, and appropriate zero padding is used to keep the feature map size constant in all layers. Each convolutional layer is followed by a ReLU layer except the last convolutional layer. Here, deep reconstruction network module can obtain an initial image with acceptable quality, which is more suitable to residual network module than cascaded residual network module [16]. The residual reconstruction network has the similar architecture as the deep reconstruction network, shown in Fig. 3, which learns the residual information between the input data and the ground truth. In our model, we set $B = 32$.

In order to train our CSRNet, we need CS measurements corresponding to each of the extracted patches. For a given measurement rate, we construct a measurement matrix, Φ_B, by first generating a random Gaussian matrix of appropriate size, followed by orthonormalizing its rows. Then, we apply $y_i = \Phi_B \times x_{\text{ver}-i}$ to obtain the set of CS measurements, where $x_{\text{ver}-i}$ is the vectorized version of an image patch x_i. Thus, an input-label pair in the training set can be represented as $\{y_i, x_i\}_i^N$. The loss function is the average reconstruction error over all the training image blocks, given by

$$L(\{W_1, W_2, W_3\}) = \frac{1}{N} \sum_{i=1}^{N} \|f_3(f_2(f_1(y_i, W_1), W_2), W_3) - x_i\|^2$$

where N is the total number of image patches in the training dataset, x_i is the ith patch, and y_i is the corresponding CS measurement. The initial reconstruction mapping, the deep reconstruction mapping, and the residual reconstruction mapping are represented as f_1, f_2, and f_3 respectively. In addition, $\{W_1, W_2, W_3\}$ are the network parameters which can be obtained in the training.

2.2 ASRNet

Our proposed ASRNet contains three modules, sampling module, initial reconstruction module, and residual reconstruction module, as shown in Fig. 4. In the sampling
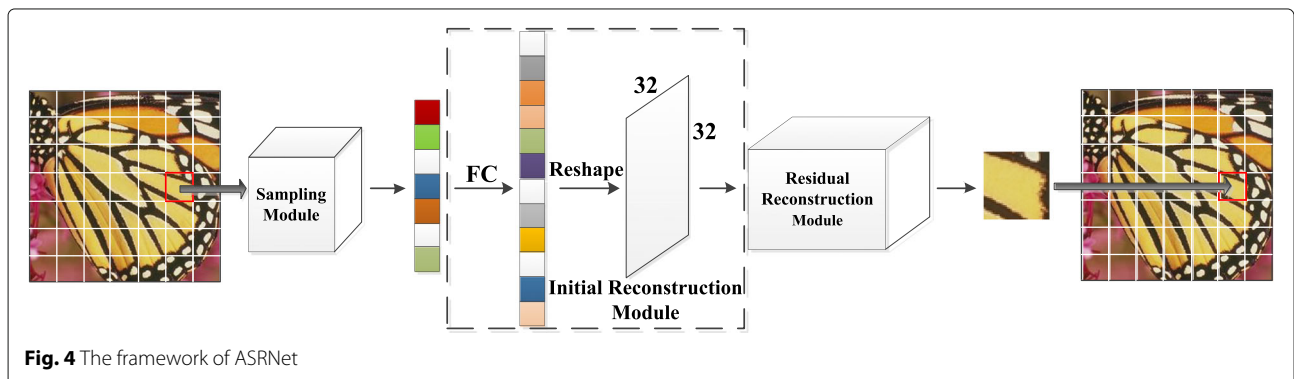

Fig. 4 The framework of ASRNet

Wang *et al. EURASIP Journal on Image and Video Processing*   (2018) 2018:77

Page 4 of 16

Table 1 PSNR valves in dB for testing image by different algorithms at the ratio MR = 0.25, 0.1, 0.04, and 0.01

Image name	Algorithm	PSNR (without applying BM3D/with using BM3D)			
		MR = 0.25	MR = 0.10	MR = 0.04	MR = 0.01
Barbara	TVAL3	24.19 / 24.20	21.88 / 22.21	18.98 / 18.98	11.94 / 11.96
	D-AMP	25.08 / 25.96	21.23 / 21.23	16.37 / 16.37	5.48 / 5.48
	ReconNet	23.25 / 23.52	21.89 / 22.50	20.38 / 21.02	18.61 / 19.08
	DR^2-Net	25.77 / 25.99	22.69 / 22.82	20.70 / 21.30	18.65 / 19.10
	CSRNet	26.17 / 26.34	22.94 / 22.95	21.27 / 21.49	19.10 / 19.21
	ASRNet	26.30 / 26.43	24.34 / 24.35	23.48 / 23.54	21.40 / 21.52
Fingerprint	TVAL3	22.70 / 22.71	18.69 / 18.70	16.04 / 16.05	10.35 / 10.37
	D-AMP	25.17 / 23.87	17.15 / 16.88	13.82 / 14.00	4.66 / 4.73
	ReconNet	25.57 / 25.13	20.75 / 20.97	16.91 / 16.96	14.82 / 14.88
	DR^2-Net	27.65 / 27.75	22.03 / 22.45	17.40 / 17.47	14.73 / 14.95
	CSRNet	27.22 / 27.49	21.64 / 21.91	17.59 / 17.68	15.11 / 15.18
	ASRNet	28.82 / 29.23	26.25 / 26.83	20.98 / 21.45	16.20 / 16.21
Flinstones	TVAL3	24.05 / 24.07	18.88 / 18.92	14.88 / 14.91	9.75 / 9.77
	D-AMP	25.02 / 24.45	16.94 / 16.82	12.93 / 13.09	4.33 / 4.34
	ReconNet	22.45 / 22.59	18.92 / 19.18	16.30 / 16.56	13.96 / 14.08
	DR^2-Net	26.19 / 26.77	21.09 / 21.46	16.93 / 17.05	14.01 / 14.18
	CSRNet	25.46 / 25.47	20.52 / 20.82	17.29 / 17.41	14.32 / 14.39
	ASRNet	26.93 / 27.40	24.01 / 24.56	19.78 / 20.08	16.30 / 16.39
Lena	TVAL3	28.67 / 28.71	24.16 / 24.18	19.46 / 19.47	11.87 / 11.89
	D-AMP	28.00 / 27.41	22.51 / 22.47	16.52 / 16.86	5.73 / 5.96
	ReconNet	26.54 / 26.53	23.83 / 24.47	21.28 / 21.82	17.87 / 18.05
	DR^2-Net	29.42 / 29.63	25.39 / 25.77	22.13 / 22.73	17.97 / 18.40
	CSRNet	29.55 / 29.70	25.72 / 25.97	22.89 / 23.17	19.11 / 19.20
	ASRNet	30.65 / 30.89	28.54 / 28.78	25.74 / 25.93	21.74 / 21.93
Monarch	TVAL3	27.77 / 27.77	21.16 / 21.25	16.73 / 16.73	11.09 / 11.11
	D-AMP	26.39 / 26.55	19.00 / 18.96	14.57 / 14.57	6.20 / 6.20
	ReconNet	24.31 / 25.06	21.10 / 21.51	18.19 / 18.32	15.39 / 15.49
	DR^2-Net	27.95 / 28.31	23.10 / 23.56	18.93 / 19.23	15.33 / 15.50
	CSRNet	27.98 / 28.37	22.99 / 23.25	19.41 / 19.60	15.42 / 15.46
	ASRNet	29.29 / 29.60	27.17 / 27.50	23.23 / 23.49	17.74 / 17.85
Parrots	TVAL3	27.17 / 27.24	23.13 / 23.16	18.88 / 18.90	11.44 / 11.46
	D-AMP	26.86 / 26.99	21.64 / 21.64	15.78 / 15.78	5.09 / 5.09
	ReconNet	25.59 / 26.22	22.63 / 23.23	20.27 / 21.06	17.63 / 18.30
	DR^2-Net	28.73 / 29.10	23.94 / 24.30	21.16 / 21.85	18.01 / 18.41
	CSRNet	28.86 / 29.05	24.79 / 25.01	22.16 / 22.31	19.50 / 19.61
	ASRNet	29.61 / 29.80	27.68 / 27.85	24.52 / 24.67	21.87 / 22.01
Boats	TVAL3	28.81 / 28.81	23.86 / 23.94	19.20 / 19.20	11.86 / 11.88
	D-AMP	29.26 / 29.26	21.90 / 21.87	16.01 / 16.01	5.34 / 5.34

Wang *et al. EURASIP Journal on Image and Video Processing* (2018) 2018:77

Page 5 of 16

Table 1 PSNR valves in dB for testing image by different algorithms at the ratio MR = 0.25, 0.1, 0.04, and 0.01 (*Continued*)

Image name	Algorithm	PSNR (without applying BM3D/with using BM3D)			
		MR = 0.25	MR = 0.10	MR = 0.04	MR = 0.01
	ReconNet	27.30 / 27.35	24.15 / 24.10	21.36 / 21.62	18.49 / 18.83
	DR^2-Net	30.09 / 30.30	25.58 / 25.90	22.11 / 22.50	18.67 / 18.95
	CSRNet	30.14 / 30.36	25.65 / 25.80	22.38 / 22.55	18.99 / 19.09
	ASRNet	31.28 / 31.64	28.86 / 29.17	25.52 / 25.72	21.53 / 21.69
Cameraman	TVAL3	25.69 / 25.70	21.91 / 21.92	18.30 / 18.33	11.97 / 12.00
	D-AMP	24.41 / 24.54	20.35 / 20.35	15.11 / 15.11	5.64 / 5.64
	ReconNet	23.15 / 23.59	21.28 / 21.66	19.26 / 19.72	17.11 / 17.49
	DR^2-Net	25.62 / 25.90	22.46 / 22.74	19.84 / 20.30	17.08 / 17.34
	CSRNet	25.85 / 26.15	22.29 / 22.53	20.23 / 20.38	17.75 / 17.90
	ASRNet	26.46 / 22.66	25.00 / 25.13	22.74 / 22.88	19.77/ 19.89
Foreman	TVAL3	35.42 / 35.54	28.69 / 28.74	20.63 / 20.65	10.97 / 11.01
	D-AMP	35.45 / 34.04	25.51 / 25.58	16.27 / 16.78	3.84 / 3.83
	ReconNet	29.47 / 30.78	27.09 / 28.59	23.72 / 24.60	20.04 / 20.33
	DR^2-Net	33.53 / 34.28	29.20 / 30.18	25.34 / 26.33	20.59 / 21.08
	CSRNet	34.89 / 35.10	30.96 / 31.35	27.78 / 28.18	23.12 / 23.32
	ASRNet	35.85 / 36.19	33.79 / 34.09	30.56 / 30.78	25.77 / 26.14
House	TVAL3	32.08 / 32.13	26.29 / 26.32	20.94 / 20.96	11.86 / 11.90
	D-AMP	33.64 / 32.68	24.55 / 24.53	16.91 / 17.37	5.00 / 5.02
	ReconNet	28.46 / 29.19	26.69 / 26.66	22.58 / 23.18	19.31 / 19.52
	DR^2-Net	31.83 / 32.52	27.53 / 28.40	23.92 / 24.70	19.61 / 19.99
	CSRNet	32.46 / 33.05	28.24 / 28.68	24.55 / 24.85	20.67 / 20.79
	ASRNet	33.44 / 33.84	31.47 / 31.87	27.82 / 28.21	23.13 / 23.31
Peppers	TVAL3	29.62 / 29.65	22.64 / 22.65	18.21 / 18.22	11.35 / 11.36
	D-AMP	29.84 / 28.58	21.39 / 21.37	16.13 / 16.46	5.79 / 5.85
	ReconNet	24.77 / 25.16	22.15 / 22.67	19.56 / 20.00	16.82 / 16.96
	DR^2-Net	28.49 / 29.10	23.73 / 24.28	20.32 / 20.78	16.90 / 17.11
	CSRNet	28.58 / 29.19	24.35 / 24.65	21.18 / 21.51	17.61 / 17.67
	ASRNet	29.72 / 30.18	27.03 / 27.37	24.03 / 24.32	20.17 / 20.33
Mean PSNR	TVAL3	27.84 / 27.87	22.84 / 22.86	18.39 / 18.40	11.31 / 11.34
	D-AMP	28.17 / 27.67	21.14 / 21.09	15.49 / 15.67	5.19 / 5.23
	ReconNet	25.54 / 25.92	22.68 / 23.23	19.99 / 20.44	17.27 / 17.55
	DR^2-Net	28.66 / 29.06	24.32 / 24.71	20.80 / 21.29	17.44 / 17.80
	CSRNet	28.83 / 29.11	24.55 / 24.81	21.52 / 21.74	18.25 / 18.35
	ASRNet	29.85 / 30.17	27.65 / 27.96	24.40 / 24.65	20.51 / 20.66

"MEAN PSNR" is the mean PSNR values among all 11 testing images

module, we use a fully connected layer to imitate the traditional compressed sampling process. And the process of compressed sampling is expressed as $y_i = \Phi_B x_i$ in traditional Block-CS. If the image is divided into B×B blocks, the input of the fully connected layer is a $B^2 \times 1$ vector. For the sampling ratio α, we can obtain $n_B = B^2 \times \alpha$ sampling measurements.

The initial reconstruction module and residual reconstruction module are matching with the sampling module. The initial reconstruction module takes those sampling

Wang *et al. EURASIP Journal on Image and Video Processing* (2018) 2018:77

Page 6 of 16

Table 2 SSIM valves in dB for testing image by different algorithms at the ratio MR = 0.25, 0.1, 0.04, and 0.01

Image name	Algorithm	SSIM (without applying BM3D)			
		MR = 0.25	MR = 0.10	MR = 0.04	MR = 0.01
Barbara	ReconNet	0.6829	0.5732	0.4803	0.3712
	DR^2-Net	0.7991	0.6364	0.5133	0.3822
	CSRNet	0.8024	0.6312	0.5275	0.3957
	ASRNet	0.8075	0.7086	0.6213	0.4665
Fingerprint	ReconNet	0.9505	0.8026	0.4918	0.1656
	DR^2-Net	0.9672	0.8576	0.5491	0.1843
	CSRNet	0.9635	0.8259	0.5278	0.1802
	ASRNet	0.9797	0.9579	0.7938	0.1818
Flinstones	ReconNet	0.8553	0.6889	0.4947	0.2758
	DR^2-Net	0.9279	0.7942	0.5536	0.2959
	CSRNet	0.9174	0.7765	0.5743	0.2965
	ASRNet	0.9516	0.9262	0.7735	0.4408
Lena	ReconNet	0.7784	0.6546	0.5650	0.4390
	DR^2-Net	0.8540	0.7303	0.6244	0.4529
	CSRNet	0.8632	0.7508	0.6471	0.4872
	ASRNet	0.8871	0.8398	0.7440	0.5684
Monarch	ReconNet	0.7808	0.6494	0.5199	0.3767
	DR^2-Net	0.8682	0.7401	0.5783	0.3899
	CSRNet	0.8691	0.7419	0.5896	0.4032
	ASRNet	0.8974	0.8618	0.7506	0.4769
Parrots	ReconNet	0.8099	0.7142	0.6315	0.5324
	DR^2-Net	0.8677	0.7709	0.6741	0.5615
	CSRNet	0.8868	0.8032	0.7180	0.6097
	ASRNet	0.9019	0.8730	0.7989	0.6790
Boats	ReconNet	0.7838	0.6454	0.5277	0.4063
	DR^2-Net	0.8612	0.7281	0.5876	0.4256
	CSRNet	0.8628	0.7198	0.5784	0.4365
	ASRNet	0.8842	0.8266	0.6937	0.5054
Cameraman	ReconNet	0.7165	0.6193	0.5317	0.4495
	DR^2-Net	0.7935	0.6872	0.5906	0.4777
	CSRNet	0.8043	0.6846	0.6048	0.5053
	ASRNet	0.8213	0.7932	0.7014	0.5696
Foreman	ReconNet	0.8469	0.7698	0.6802	0.5810
	DR^2-Net	0.9028	0.8360	0.7506	0.6220
	CSRNet	0.9172	0.8598	0.7813	0.6541
	ASRNet	0.9280	0.9048	0.8470	0.7247
House	ReconNet	0.7832	0.6933	0.6121	0.5286

Table 2 SSIM valves in dB for testing image by different algorithms at the ratio MR = 0.25, 0.1, 0.04, and 0.01 (*Continued*)

Image name	Algorithm	SSIM (without applying BM3D)			
		MR = 0.25	MR = 0.10	MR = 0.04	MR = 0.01
	DR^2-Net	0.8459	0.7617	0.6753	0.5540
	CSRNet	0.8593	0.7785	0.6943	0.5805
	ASRNet	0.8751	0.8434	0.7695	0.6296
Peppers	ReconNet	0.7488	0.6351	0.5315	0.4222
	DR^2-Net	0.8232	0.7042	0.5832	0.4365
	CSRNet	0.8271	0.7219	0.6195	0.4747
	ASRNet	0.8605	0.8386	0.7549	0.5607
Mean SSIM	ReconNet	0.7942	0.6769	0.5515	0.4135
	DR^2-Net	0.8646	0.7497	0.6073	0.4348
	CSRNet	0.8703	0.7540	0.6239	0.4567
	ASRNet	0.8904	0.8522	0.7499	0.5276

"MEAN SSIM" is the mean SSIM values among all 11 testing images

measurements as input and outputs a B×B-sized preliminary reconstructed image. Similar to sampling module, we also use a fully connected layer to imitate the traditional initial reconstruction process, which can be presented by $\tilde{x}_j = \tilde{\phi}_B \times y_j$. In our design, the $\tilde{\phi}_B$ can be learned automatically instead of computing by the complicated MMSE linear estimation. The residual reconstruction module is similar as the residual reconstruction module in CSRNet, shown in Fig. 3. The output of the residual reconstruction module is the final output of the network.

Given the original image x_i, our goal is to obtain the highly compressed measurement y_j with the compressed sampling module and then accurately recover it to the original image x_j with reconstruction module. Since the sampling module, the initial reconstruction module, and the residual reconstruction module form an end-to-end network, they can be trained together and do not need to be concerned with what the compressed measurement is in training. Therefore, the input and the label are all the image itself for training our ASRNet. Following most of deep learning-based image restoration

Table 3 Time(in seconds) for reconstruction a single 256 × 256 image

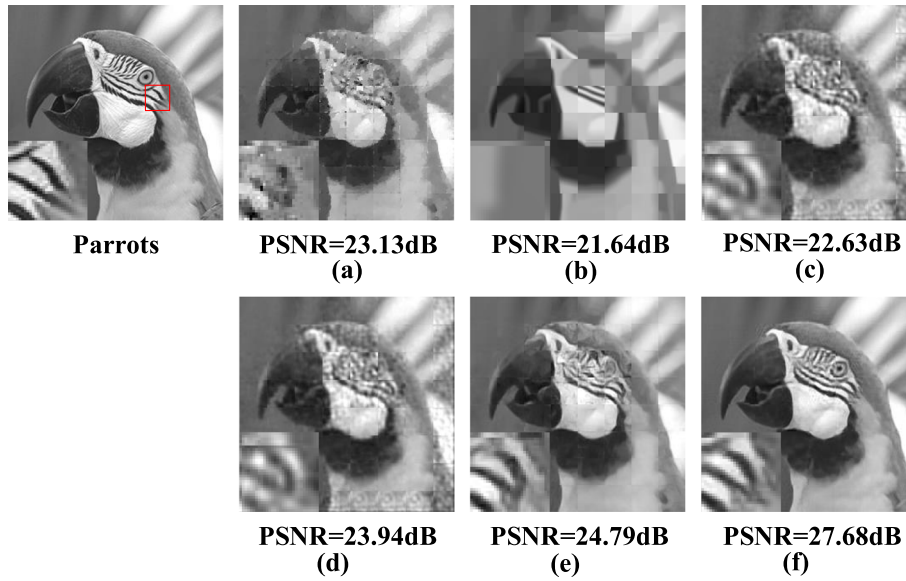| Models	MR = 0.25	MR = 0.10	MR = 0.04	MR = 0.01
ReconNet	0.5376	0.5366	0.5415	0.5508
DR^2-Net	1.2879	1.2964	1.3263	1.3263
CSRNet	0.5355	0.5375	0.5464	0.5366
ASRNet	0.3038	0.2984	0.3005	0.3025

Fig. 5 The reconstruction results of Parrots at the measurement rate of 0.1 without BM3D. **a** TVAL3. **b** DAMP. **c** ReconNet. **d** DR²-Net. **e** CSRNet. **f** ASRNet

methods, the mean square error is adopted as the cost function of our network. The optimization objective is represented as

$$L(\{W_4, W_5, W_6\}) = \frac{1}{N} \sum_{i=1}^{N} \|f_6(f_5(f_4(x_i, W_1), W_2), W_3) - x_i\|^2$$

where $\{W_4, W_5, W_6\}$ are the network parameters needed to be trained, f_4 is the sampling, and f_5 and f_6 correspond the initial reconstruction mapping and residual

reconstruction mapping respectively. It should be noted that we train the compressed sampling network and the reconstruction network together, but they can be used independently.

3 Results and discussion

In this section, we evaluate the performance of the proposed methods for CS reconstruction. We will firstly introduce the details during our training and testing.
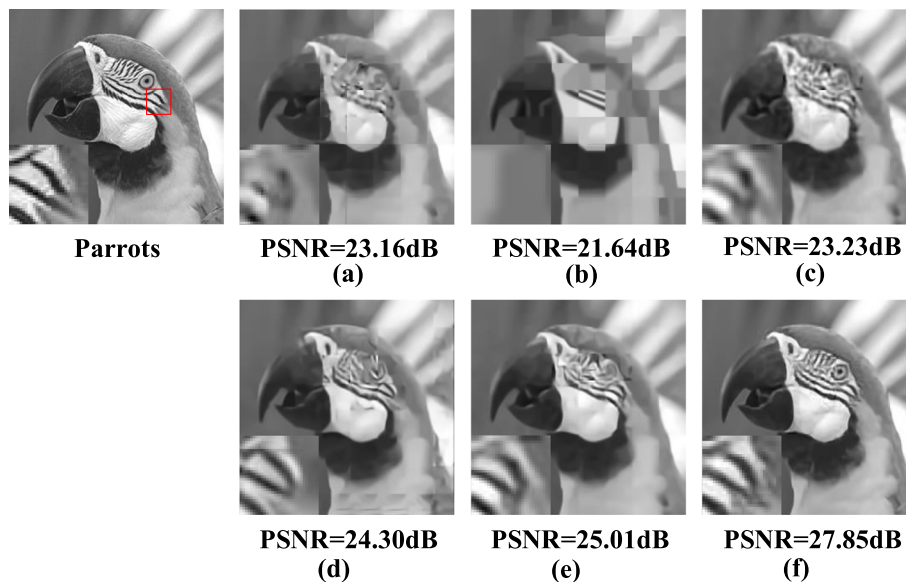
Fig. 6 The reconstruction results of Parrots at the measurement rate of 0.1 with BM3D. **a** TVAL3. **b** DAMP. **c** ReconNet. **d** DR²-Net. **e** CSRNet. **f** ASRNet
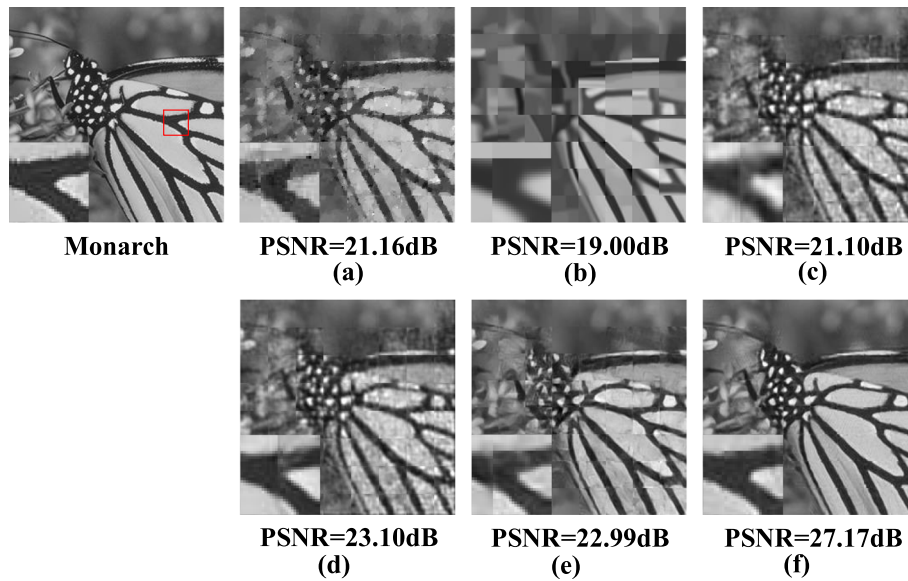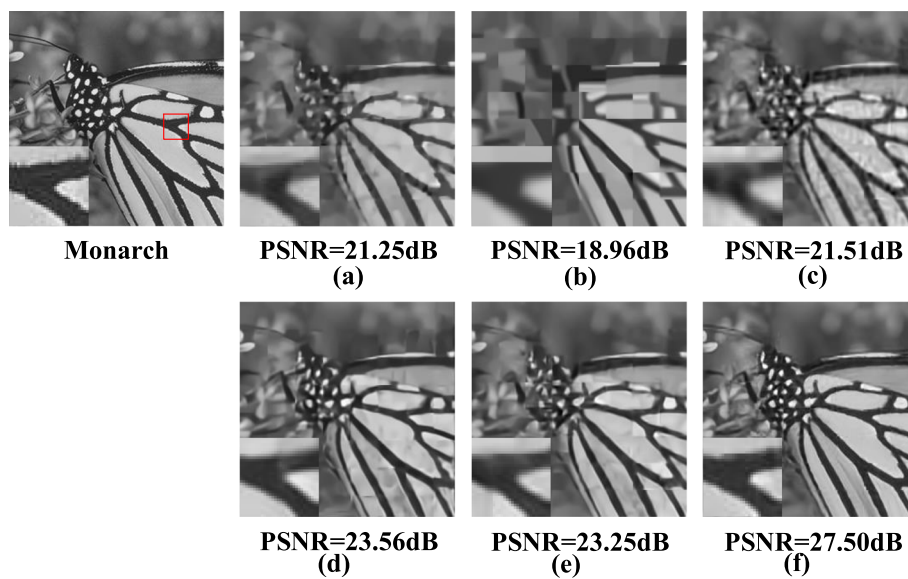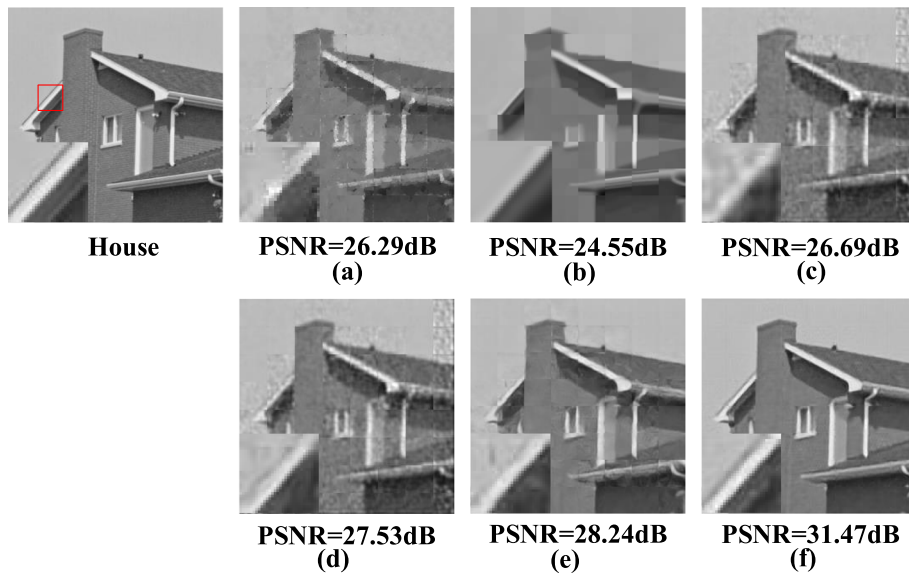
Fig. 7 The reconstruction results of Monarch at the measurement rate of 0.1 without BM3D. **a** TVAL3. **b** DAMP. **c** ReconNet. **d** DR^2-Net. **e** CSRNet. **f** ASRNet

Then, we show the quantitative and qualitative comparisons with four state-of-the-art methods.

3.1 Training

The dataset used in our training is the set of 91 images in the [14]. The set 5 from [14] constitutes to be our validation set. We only use the luminance component of the images. We uniformly extract patches of size 32×32 from these images with a stride equal 14 for training and 21 for validation to form the training dataset of 22,144 patches and the validation dataset which contains 1112 patches. Both CSRNet and ASRNet use the same dataset. We train the proposed networks with different measurement rates (MR) = 0.25, 0.10, 0.04, and 0.01. The Caffe is used to train the proposed model.

Fig. 8 The reconstruction results of Monarch at the measurement rate of 0.1 with BM3D. **a** TVAL3. **b** DAMP. **c** ReconNet. **d** DR^2-Net. **e** CSRNet. **f** ASRNet

Wang *et al. EURASIP Journal on Image and Video Processing* (2018) 2018:77

Page 9 of 16

Fig. 9 The reconstruction results of House at the measurement rate of 0.1 without BM3D. **a** TVAL3. **b** DAMP. **c** ReconNet. **d** DR^2-Net. **e** CSRNet. **f** ASRNet

3.2 Comparison with existing methods

3.2.1 Objective quality comparisons

Our proposed algorithm is compared with four representative CS recovery methods, TVAL3 [8], D-AMP [5], ReconNet [14], and DR^2-Net [16]. The first two belong to traditional optimization-based methods, while the last two are recent network-based methods. For the simulated data in our experiments, we evaluate the proposed methods on the same test images as in [14], which consists of 11 grayscale images. Here, nine images have size

of 256×256 and two images are 512×512. We compute the PSNR value for total 11 images, and the results are shown in Table 1. We use the BM3D [18] as the denoiser to remove the artifacts resulting due to patch processing. It is obvious to see that ASRNet can achieve more than 1 dB gain, as compared with CSRNet. We add SSIM comparison between our proposed networks and network-based methods, ReconNet and DR^2-Net, as shown in Table 2. From Tables 1 and 2, it can be found that our proposed CSRNet and ASRNet outperform other
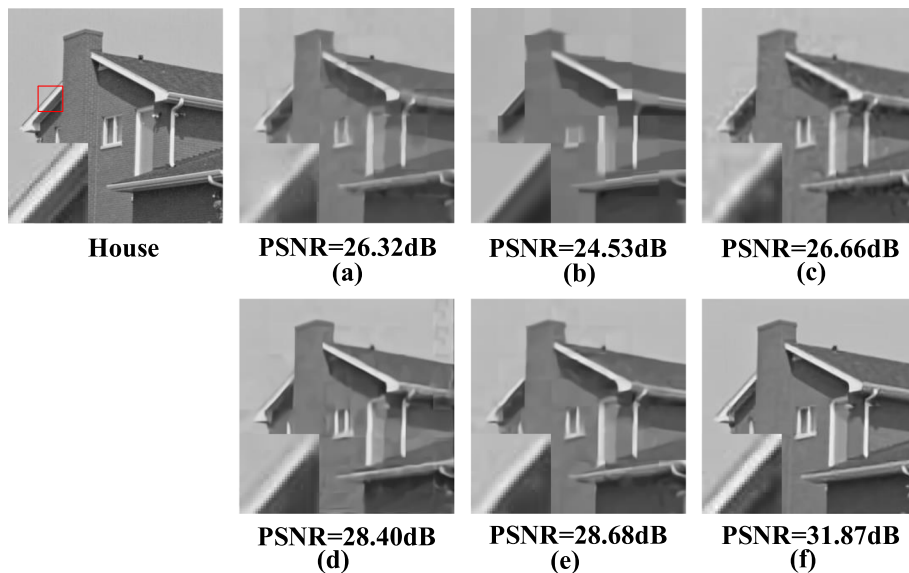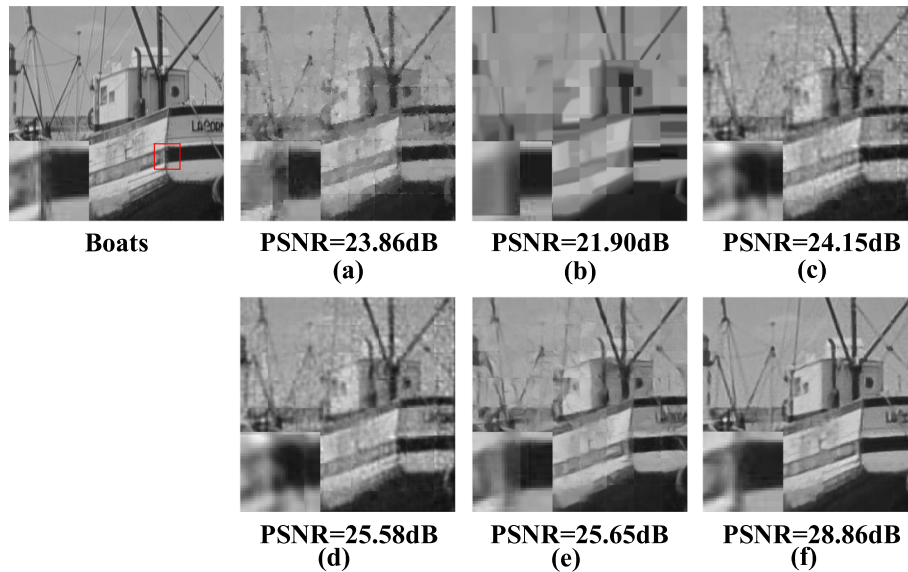

Fig. 10 The reconstruction results of House at the measurement rate of 0.1 with BM3D. **a** TVAL3. **b** DAMP. **c** ReconNet. **d** DR^2-Net. **e** CSRNet. **f** ASRNet

Wang *et al. EURASIP Journal on Image and Video Processing* (2018) 2018:77

Page 10 of 16

Fig. 11 The reconstruction results of Boats at the measurement rate of 0.1 without BM3D. **a** TVAL3. **b** DAMP. **c** ReconNet. **d** DR^2-Net. **e** CSRNet. **f** ASRNet

algorithms under each measurement rates, especially at 0.04 and 0.01. In addition, the performance of our methods decreases slowly compared to other algorithms with the measurement rate down.

3.2.2 Time complexity

The time complexity is a key factor for image compressive sensing. In the progress of reconstruction, the network-based algorithms are much faster than traditional iterative reconstruction methods, so we only compare the time complexity with ReconNet and DR^2-Net. Table 3 shows the average time for reconstructing nine sized 256×256 images of those network-based methods.

From the Tables 1, 2, and 3, we can observe that the proposed CSRNet and ASRNet outperform the Recon-Net and DR^2-Net in terms of PSNR, SSIM, and time complexity. And our ASRNet obtains the best performance in all objective quality assessments. Notably, ASR-Net run fastest which is very important for real-time applications.
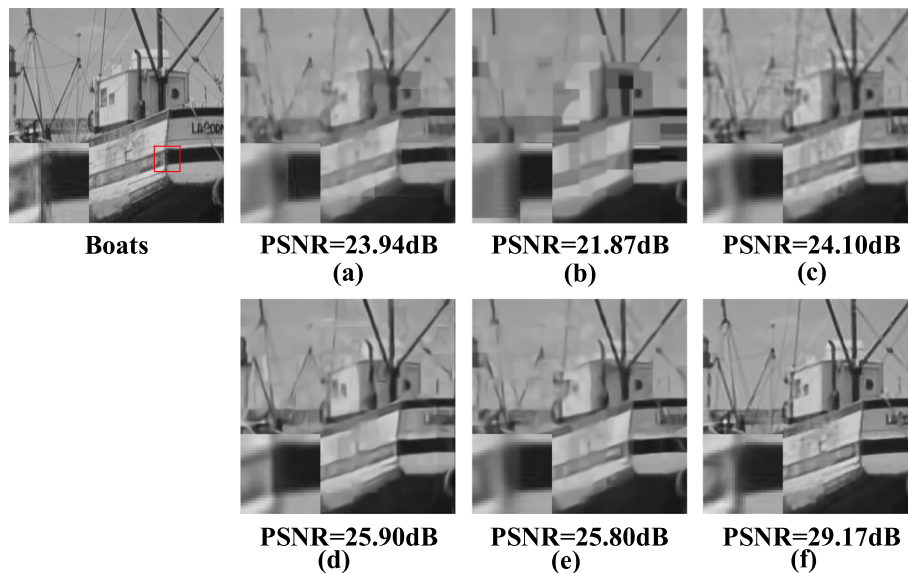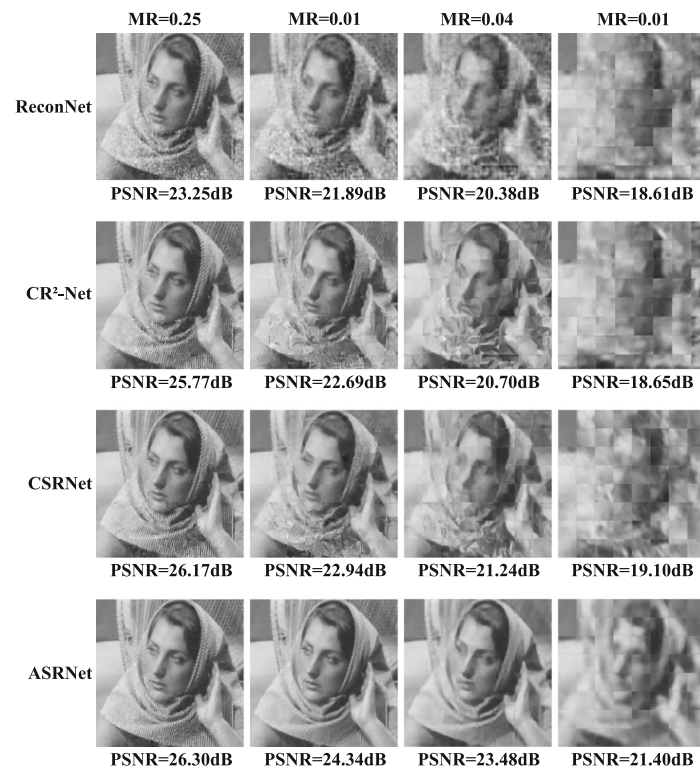

Fig. 12 The reconstruction results of Boats at the measurement rate of 0.1 with BM3D. **a** TVAL3. **b** DAMP. **c** ReconNet. **d** DR^2-Net. **e** CSRNet. **f** ASRNet

Wang *et al. EURASIP Journal on Image and Video Processing*   (2018) 2018:77

Page 11 of 16

	MR=0.25	MR=0.01	MR=0.04	MR=0.01
ReconNet				
	PSNR=23.25dB	PSNR=21.89dB	PSNR=20.38dB	PSNR=18.61dB
CR²-Net				
	PSNR=25.77dB	PSNR=22.69dB	PSNR=20.70dB	PSNR=18.65dB
CSRNet				
	PSNR=26.17dB	PSNR=22.94dB	PSNR=21.24dB	PSNR=19.10dB
ASRNet				
	PSNR=26.30dB	PSNR=24.34dB	PSNR=23.48dB	PSNR=21.40dB

Fig. 13 The reconstruction results of Barbara at the measurement rate of 0.25, 0.1, 0.04, and 0.01 without BM3D

	MR=0.25	MR=0.01	MR=0.04	MR=0.01
ReconNet				
	PSNR=23.52dB	PSNR=22.50dB	PSNR=21.02dB	PSNR=19.08dB
CR²-Net				
	PSNR=25.99dB	PSNR=22.82dB	PSNR=21.30dB	PSNR=19.10dB
CSRNet				
	PSNR=26.30dB	PSNR=22.95dB	PSNR=21.47dB	PSNR=19.17dB
ASRNet				
	PSNR=26.43dB	PSNR=24.35dB	PSNR=23.54dB	PSNR=21.52dB

Fig. 14 The reconstruction results of Barbara at the measurement rate of 0.25, 0.1, 0.04, and 0.01 with BM3D
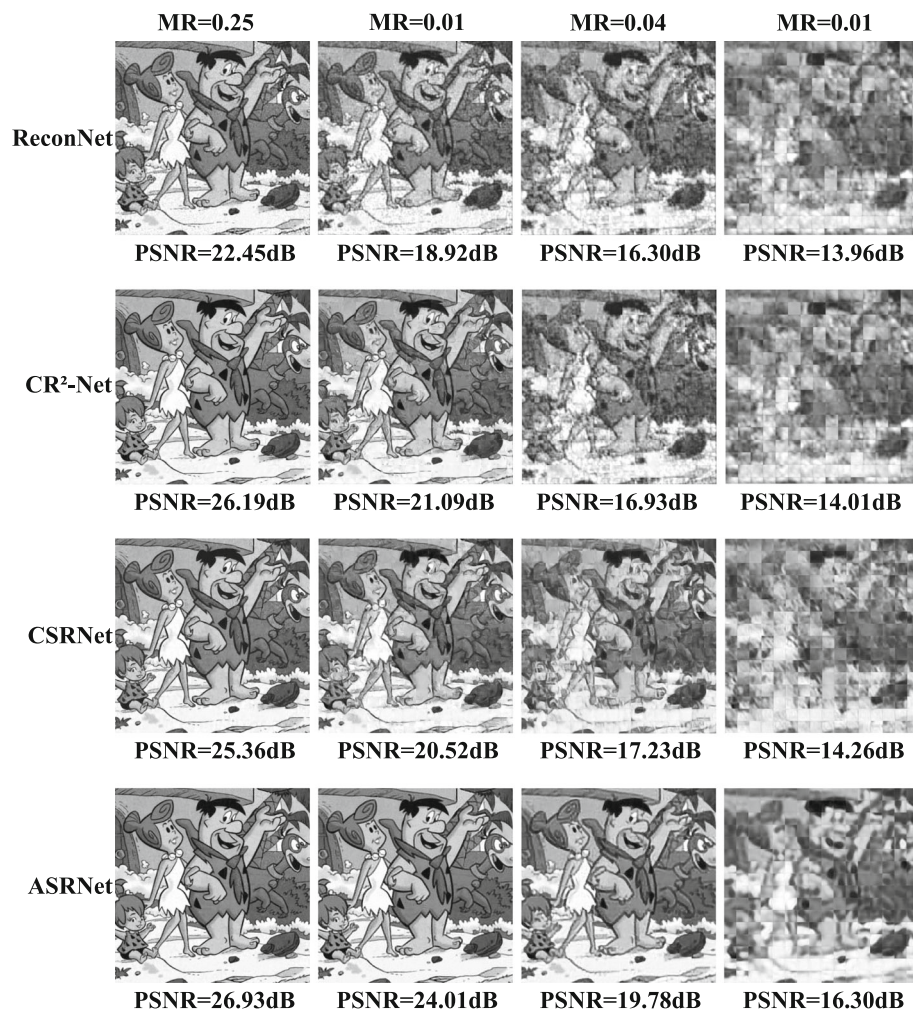
Fig. 15 The reconstruction results of Flinstones at the measurement rate of 0.25, 0.1, 0.04, and 0.01 without BM3D

3.2.3 Visual quality comparisons

Our proposed algorithm is compared with four representative CS recovery methods, TVAL3, D-AMP, ReconNet, and DR^2-Net in visual. Figures 5 and 6 show the visual comparisons of Parrots in the case of measurement rate = 0.1 with and without BM3D respectively. It is obvious that the proposed CSRNet and ASRNet are able to reconstruct more details and sharper, which offers better visual reconstruction results than other network-based algorithms. The other three groups are shown in Figs. 7, 8, 9, 10, 11, and 12. The test images under different rates with or without BM3D are shown in the Figs. 13, 14, 15, and 16. We can see that our proposed CSRNet and ASRNet outperforms ReconNet and DR^2-Net at each measurement rate.

3.3 Evaluation on our proposed architectures

In order to verify the innovation and rationality of our networks' architectures in more detail, we add a comparison between the intermediate outputs and the final outputs of our methods in objective and subjective quality. Apart from the above four MR, we additionally train the models of CSRNet and ASRNet at the MR = 0.2 and 0.15. We calculate the mean PSNR and SSIM values of the total 11 test images at each measurement rate, as shown in Table 4. The CSRNet-i means the intermediate output of the deep reconstruction module in the CSRNet, and the ASRNet-i represents the intermediate output of the initial reconstruction module in the ASRNet. From the results shown in Table 4, the final outputs of CSRNet and ASRNet both perform better than their intermediate outputs at each measurement rate. As shown in Figs. 17 and 18, we respectively give the intermediate and final CSRNet subjective evaluation of Cameraman, House, Monarch, and Parrots at MR = 0.20 and 0.10. Figures 19 and 20 show the intermediate and final ASRNet subjective evaluation of Boats, Cameraman, Peppers, and Monarch at MR = 0.04 and 0.10. Compared to intermediate results, our final results
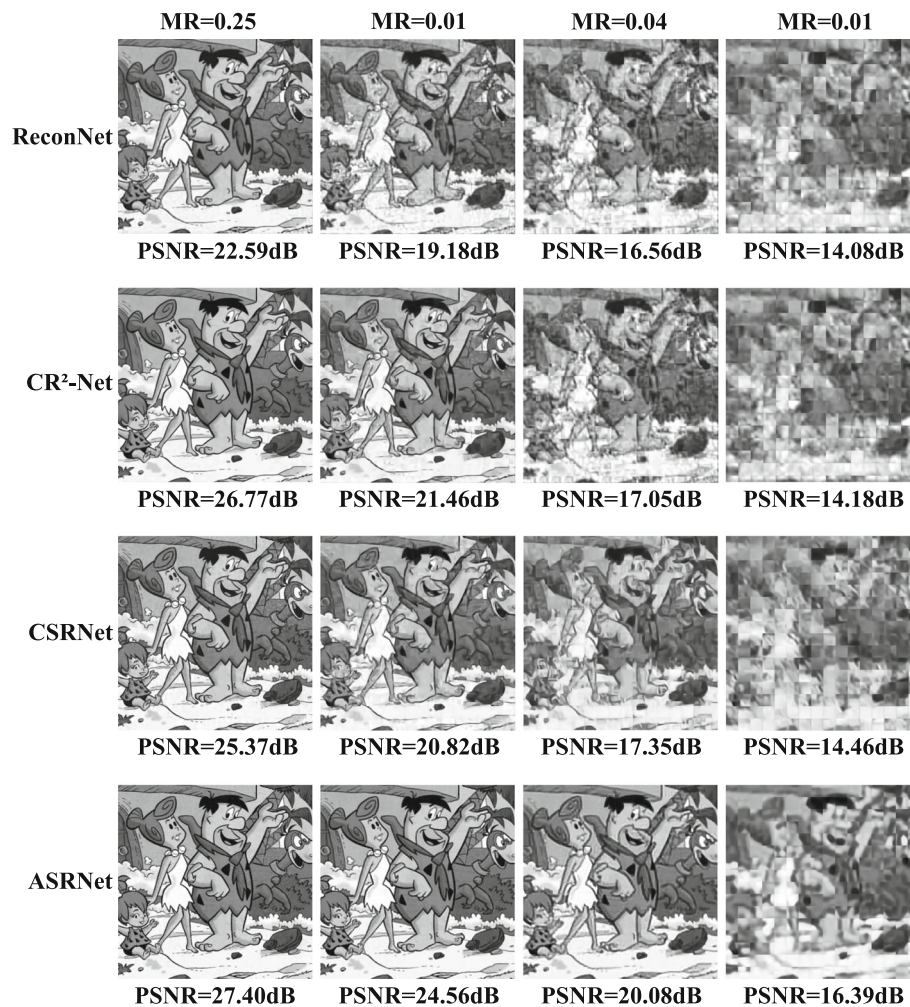
Fig. 16 The reconstruction results of Flinstones at the measurement rate of 0.25, 0.1, 0.04, and 0.01 with BM3D

express more natural textures and details. All final results outperform previous intermediate results substantially in terms of image quality. It is intuitively confirmed that our proposed networks are reasonable, stable, and reliable.

4 Conclusion

In this paper, two cascaded reconstructed networks are proposed for different CS sampling methods. In most previous works, the sample matrix is a random matrix in CS process. And the first network is a compatibly

sampling reconstruction network (CSRNet), which can reconstruct high-quality image from its compressively sensed measurement sampled by a traditional random matrix. The second network is adaptively sampling reconstruction network (ASRNet), by matching automatically sampling module with corresponding residual reconstruction module. And the sampling module could perfectly solve the problem of sampling efficiency in compressive sensing. Experimental results show that the proposed networks, CSRNet and ASRNet, have achieved the

Table 4 The mean PSNR/SSIM values of 11 test images without applying BM3D

Models	MR = 0.25	MR = 0.20	MR = 0.15	MR = 0.10	MR = 0.04	MR = 0.01
CSRNet-i	27.53/0.8322	24.70/0.7554	24.32/0.7405	23.57/0.7068	21.27/0.6085	18.24/0.4401
CSRNet	28.83/0.8703	25.42/0.7847	25.27/0.7818	24.55/0.7540	21.52/0.6239	18.25/0.4567
ASRNet-i	28.48/0.8527	27.39/0.8343	26.81/0.8208	26.76/0.8262	23.89/0.7240	20.37/0.5187
ASRNet	29.85/0.8904	29.19/0.8842	28.30/0.8668	27.65/0.8521	24.40/0.7499	20.51/0.5276

Wang *et al. EURASIP Journal on Image and Video Processing* (2018) 2018:77
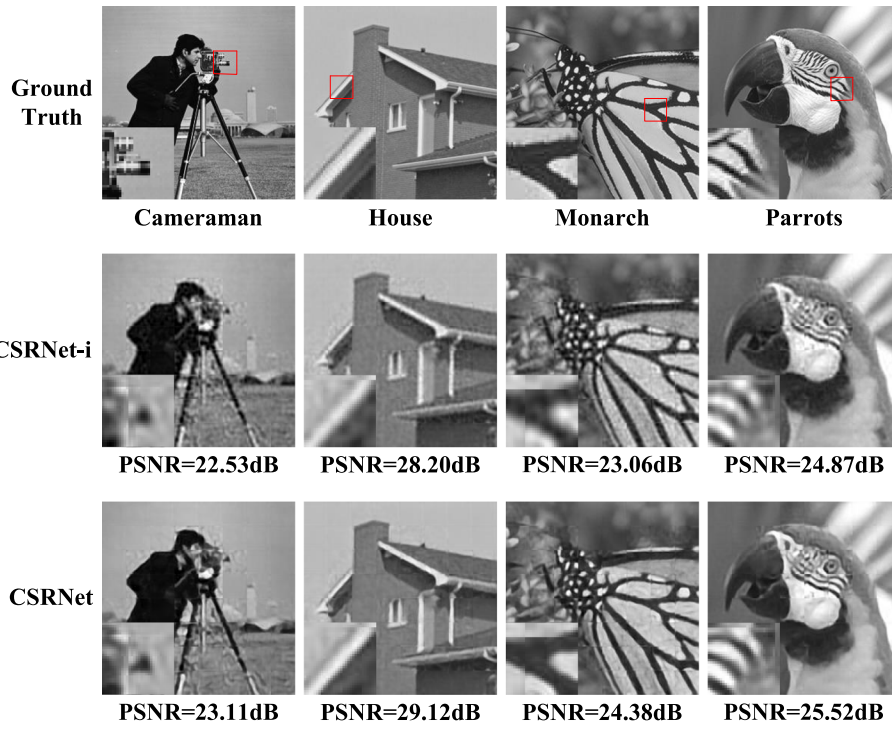
Page 14 of 16

Fig. 17 The intermediate and final reconstruction results of CSRNet at the measurement rate 0.20
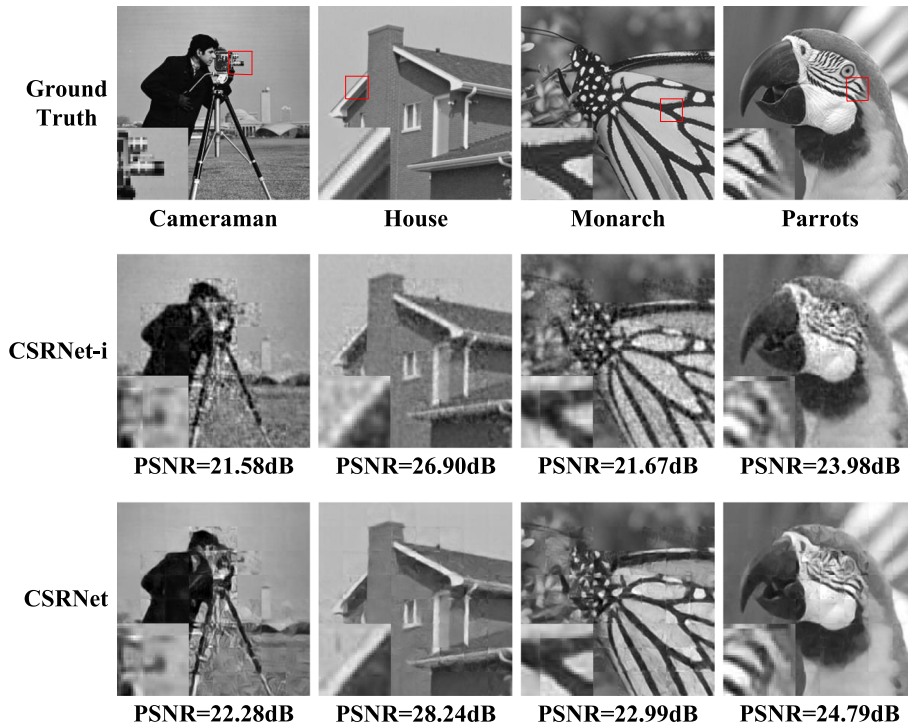

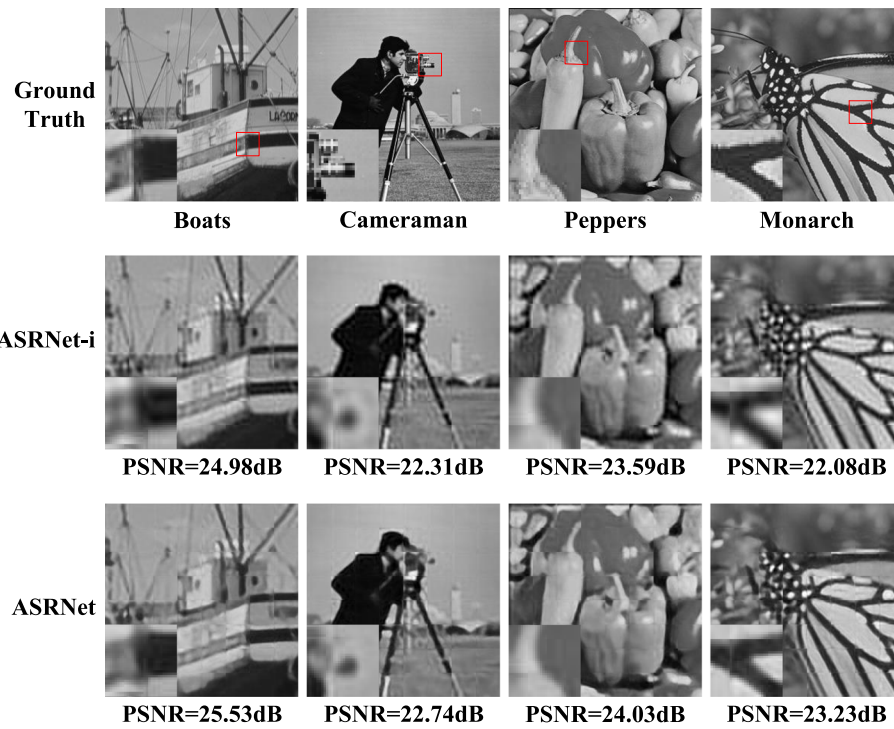**Fig. 18** The intermediate and final reconstruction results of CSRNet at the measurement rate 0.10

Fig. 19 The intermediate and final reconstruction results of ASRNet at the measurement rate 0.04
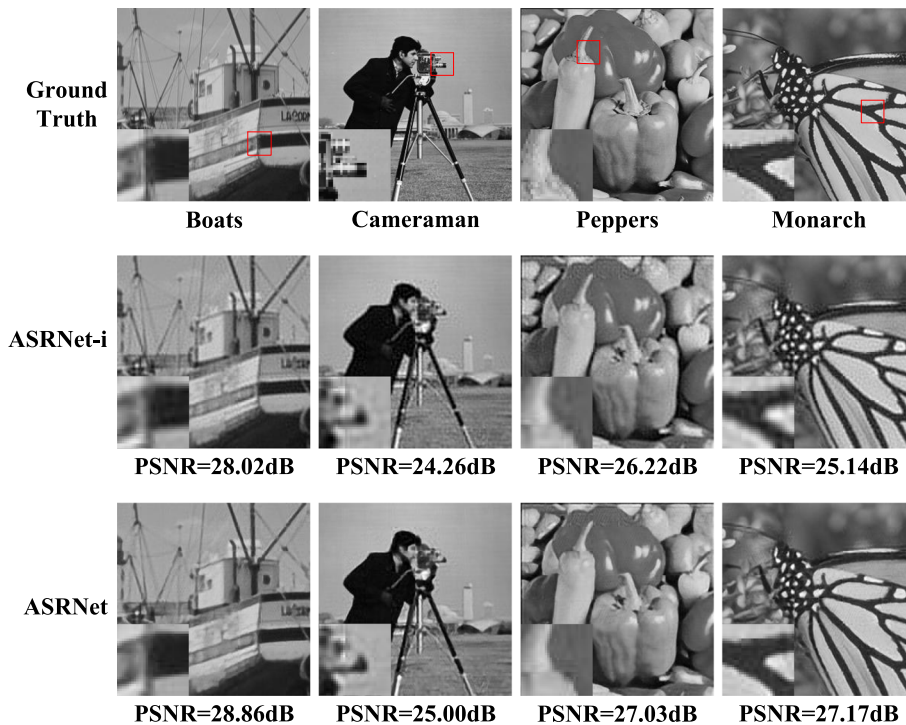

Fig. 20 The intermediate and final reconstruction results of ASRNet at the measurement rate 0.10

Wang *et al. EURASIP Journal on Image and Video Processing*   (2018) 2018:77

Page 16 of 16

significant improvements in reconstruction results over the traditional and neural network-based CS reconstruction algorithms both in terms in quality and time complexity. Furthermore, ASRNet can achieve more than 1 dB gain, as compared with CSRNet.

Abbreviations
ASRNet: Adaptively sampling reconstruction network; CS: Compressive sensing; CSRNet: Compatibly sampling reconstruction network

Authors' contributions
YW completed most of the text and implementation of the algorithm. HB and LZ directed this work and contributed to the revisions. YZ reviewed and revised the manuscript. All authors read and approved the final manuscript.

Competing interests
The authors declare that they have no competing interests.

Publisher's Note
Springer Nature remains neutral with regard to jurisdictional claims in published maps and institutional affiliations.

References
1. D.L. Donoho, Compressed sensing. IEEE Trans. Inf. Theory. **52**(4), 1289–1306 (2006)
2. G. Lu, Block compressed sensing of natural images. Int. Conf. Digit. Signal Process, 403–406 (2007)
3. J.A. Tropp, Greed is good: algorithmic results for sparse approximation. IEEE Trans. Inf. Theory. **50**(10), 2231–2242 (2004)
4. D.L. Donohoa, A. Malekib, A. Montanaria, Message-passing algorithms for compressed sensing. Proc. Natl. Acad. Sci. U. S. A. **106**(45), 18914 (2009)
5. C.A. Metzler, A. Maleki, R.G. Baraniuk, From denoising to compressed sensing. IEEE Trans. Inf. Theory. **62**(9), 5117–5144 (2016)
6. Y. Xiao, J. Yang, Alternating algorithms for total variation image reconstruction from random projections. Inverse Probl. Imaging. **6**(3), 547–563 (2017)
7. M. Elad, M. Aharon, Image denoising via sparse and redundant representations over learned dictionaries. IEEE Trans. Image Process. **15**(12), 3736–3745 (2006)
8. C. Li, W. Yin, H. Jiang, Y. Zhang, An efficient augmented Lagrangian method with applications to total variation minimization. Comput. Optim. Appl. **56**(3), 507–530 (2013)
9. L. Ma, H. Bai, M. Zhang, Y. Zhao, Edge-based adaptive sampling for image block compressive sensing. Ieice Trans. Fundam. Electron. Commun. Comput. Sci. **E99.A**(11), 2095–2098 (2016)
10. H. Bai, M. Zhang, M. Liu, A. Wang, Y. Zhao, Depth image coding using entropy-based adaptive measurement allocation. Entropy. **16**(12), 6590–6601 (2014)
11. C. Dong, C.L. Chen, K. He, X. Tang, Image super-resolution using deep convolutional networks. IEEE Trans. Pattern. Anal. Mach. Intell. **38**(2), 295–307 (2016)
12. L. Zhao, J. Liang, H. Bai, A. Wang, Y. Zhao, Simultaneously color-depth super-resolution with conditional generative adversarial network. arXiv preprint arXiv:1708.09105. (2017)
13. L. Zhao, J. Liang, H. Bai, A. Wang, Y. Zhao, in *IEEE International Conference on Image Processing*. Convolutional neural network-based depth image artifact removal (IEEE International Conference on Image Processing, 2017)
14. K. Kulkarni, S. Lohit, P. Turaga, R. Kerviche, A. Ashok, ReconNet: non-iterative reconstruction of images from compressively sensed random measurements. The IEEE Conference on Computer Vision and Pattern Recognition (CVPR) (2016)
15. A. Mousavi, R.G. Baraniuk, Learning to invert: signal recovery via deep convolutional networks. IEEE International Conference on Acoustics, Speech and Signal Processing (2017)
16. H. Yao, F. Dai, D. Zhang, Y. Ma, S. Zhang, DR^2-Net: deep residual reconstruction network for image compressive sensing. The IEEE Conference on Computer Vision and Pattern Recognition (CVPR) (2017)
17. G. Nie, Y. Fu, Y. Zheng, H. Huang, Image restoration from patch-based compressed sensing measurement. The IEEE Conference on Computer Vision and Pattern Recognition (CVPR) (2017)
18. K. Dabov, A. Foi, V. Katkovnik, K. Egiazarian, Image denoising by sparse 3-d transform-domain collaborative filtering. IEEE Trans. Image Process. **16**(8), 2080–2095 (2007)